# $LiClO_4$-Doped Plasticized Chitosan as Biodegradable Polymer Gel Electrolyte for Supercapacitors

**M. Selva Kumar, D. Krishna Bhat**

*Department of Chemistry, National Institute of Technology Karnataka Surathkal, Srinivasnagar, Karnataka 575025, India*

Received 21 June 2008; accepted 7 May 2009
DOI 10.1002/app.30716
Published online 7 July 2009 in Wiley InterScience (www.interscience.wiley.com).

**ABSTRACT:** Studies on redox supercapacitors using electronically conducting polymers are of great importance for hybrid power sources and pulse power applications. In this study, electrochemical properties of a chitosan-based biodegradable polymer gel electrolyte (PGE) and a p/p polypyrrole supercapacitor fabricated using this electrolyte have been investigated. The variation of conductivity and dielectric properties of the electrolyte film with temperature has also been measured. The PGE film chosen for the study exhibited a specific conductivity of $5.5 \times 10^{-3}$ S $cm^{-1}$. The electric modulus of the electrolyte film exhibits a long tail feature indicative of good capacitance. The fabricated supercapacitor showed a fairly good specific capacitance of 120 F $g^{-1}$ and a time constant of 1 s. © 2009 Wiley Periodicals, Inc. J Appl Polym Sci 114: 2445–2454, 2009

**Key words:** gel polymer electrolyte; lithium perchlorate; chitosan; dielectric constant; supercapacitor

## INTRODUCTION

Chitosan has aroused a lot of interest in view of its applications in the industrial and biomedical sectors.[1,2] It is also the first natural polymer-chelating membrane, does not possess any pores, and also a biodegradable polymer. In its actual state, a chitosan film has very low electrical conductivity. The hydrogen atoms in the chitosan monomer are strongly bonded and cannot be mobilized under the action of an electric field. To make chitosan a proton conductor, chitosan has been dissolved in acetic acid and the solution cast to form a film.[3] The dispersed $H^+$ and $CH_3COO^-$ ions in the chitosan solvent can be mobilized on application of an electric field. If the addition of a proton donor leads to an increase in electrical conductivity, then it should be possible to produce a more ionically conducting film by increasing the hydrogen donor concentration. Good amount of effort has been harnessed to produce chitosan-based polymer electrolytes.[3–5] Solid polymer electrolytes have ionic conductivity between $10^{-8}$ and $10^{-7}$ S $cm^{-1}$, which are too low to be of use in practical devices. Efforts[6] have, therefore, been expended to enhance the ionic conductivity of polymer electrolytes. One such approach involves addition of a low-molecular-weight polar solvent[7–9] called plasticizer, to a polymer-salt system to form a polymer gel electrolyte (PGE). PGEs have good adhesive properties, liquid-like behavior, and exhibit high ionic conductivity of the order of $\sim 10^{-3}$ S $cm^{-1}$ at ambient temperatures. Nonaqueous PGEs have a wider potential window of $\sim 4$ V compared with that of $\sim 1$ V for aqueous PGEs. Electrochemical capacitors (ECs) are electrical devices with highly reversible charge-storage and delivery capabilities. ECs have properties complementary to secondary batteries and find usage in hybrid power systems, military, and medical applications.[10] ECs use both aqueous and nonaqueous electrolytes in either liquid or solid state. Solid electrolytes provide the advantages of compactness and reliability without leakage of liquid components. Depending on the charge-storage mechanism, an EC is classified as an electrochemical double-layer capacitor (EDLC) or a pesudocapacitor. Higher energy density of EDLCs, when compared with dielectric capacitors, is mainly due to the large surface area of the electrode materials, usually comprising activated carbons, aerogel or xerogel carbons, and carbon nanotubes.[11–16] DLCs have several advantages over secondary batteries, such as faster charge-discharge, longer cycle-life ($>10^5$ cycles), and higher power density. Pseudocapacitors are also called redox capacitors because of the involvement of redox reactions in the charge-storage and delivery processes. Energy storage mechanisms in pseudocapacitors involve fast faradaic reactions at or near a solid electrode surface at an appropriate potential. Redox processes often occur in conducting polymers and metal oxides making them attractive materials for pseudocapacitors.[10] Reportedly, organic

*Correspondence to:* D. K. Bhat (denthaje@gmail.com).
Contract grant sponsors: MHRD, Govt. of India (R&D project).

PGEs have been used in both lithium batteries and EDLCs[7–9] and aqueous PGEs in ECs.[17,18] But, owing to their corrosive nature, acidic electrolytes are suitable only to a limited number of electrode materials. Alkaline PGEs, such as PEO-KOH-$H_2O$[19,20] and PAA-KOH-$H_2O$,[21,22] have found applications in nickel-metal hydride batteries and EDLCs. However, an aqueous PGE, sometimes called gel ionic or wet- two-phase solid electrolytes, combines the advantageous mechanical properties of the polymer and the electrochemical properties of the liquid organic electrolyte. Gel ionic electrolytes, based on poly(methylmethacrylate),[23,24] have been proposed for lithium battery application particularly because of their beneficial effects on the stabilization of the electrode–electrolyte interface.[25] Conducting polymers are more interesting than carbons and transition metal oxides because of the following merits.[26]

(i) Conducting polymers have higher electronic conductivity than the metal oxides,
(ii) they are cheaper than some oxides, e.g., $RuO_2.xH_2O$,
(iii) they can be prepared by using electrochemical methods in a well-controlled manner,
(iv) electrochemical deposition ensures coherence and adherence to the current collecting substrates, and
(v) electrochemical deposition avoids the procedures of electrode-fabrication with suitable binders.

Among the conducting polymers, polypyrrole (PPy) is of interest because of its high electrical conductivity, good environmental stability, and rather easy synthesis. PPy can also be processed when doped with inorganic or organic acids. The electronic structure of doped conducting polymers is strongly influenced by the disorder, which arises from the inhomogeneous doping. The charge carriers generated in the process of doping by conjugated polymeric chains are generally polarons or bipolarons and contribute to conductivity by phonon-assisted hopping or tunneling.[27–29]

In view of the aforementioned discussion, we have chosen PPy electrode material and a biodegradable PGE based on $LiClO_4$-doped chitosan for fabricating a supercapacitor. Preparation and electrochemical properties of a p/p PPy supercapacitor fabricated using this gel polymer electrolyte have been evaluated and presented in this article.

## EXPERIMENTAL

### Materials

All the chemicals used are of analytical reagent grade. Chitosan (medium molecular weight) from Aldrich and sodium dodecyl sulfate (SDS) from Merck were used as such without further purification. $LiClO_4$ from Loba Chemie, India was vacuum dried at 120°C before use. Ethylene carbonate (EC) and propylene carbonate (PC) from Alfa Aesar, acetic acid from SD Fine Chemicals, India, and pyrrole from Acros Organics were used after vacuum distillation. Double distilled water was used for the preparation of aqueous solutions.

### Preparation of PGE

One gram of chitosan powder was dissolved in 100 $cm^3$ of 1% (v/v) acetic acid solution. The mixture was stirred continuously with a magnetic stirrer at room temperature until the chitosan powder was completely dissolved in the weak acid solution. For the preparation of PGE films, a suspension was made by mixing appropriate amounts of EC, PC, $LiClO_4$, and chitosan solution. The well-stirred suspension in a glass petri dish was heated at about 100°C for about 2 min. Subsequent to cooling, the resultant product was in the form of a transparent film of PGE. To arrive at appropriate composition, several PGE films were prepared by varying the quantities of EC, PC, and $LiClO_4$ with a constant quantity of chitosan. An appropriate composition was considered to be the one, which required a minimum liquid component for formation of the gel and had maximum specific conductivity. The composition thus arrived at had the mass ratio of chitosan/EC/PC/$LiClO_4$ equal to 1 : 3 : 3 : 0.4. The specific conductivity of this PGE film at room temperature was found to be $5.5 \times 10^{-3}$ S $cm^{-1}$ and thickness was 0.2 mm. The polyelectrolyte film prepared without plasticizer showed a specific conductivity of $0.8 \times 10^{-3}$ S $cm^{-1}$. The variation of conductivity with temperature for PGE films of various compositions is shown in Figure 1.

### Biodegradation study

Biodegradation behavior of the PGE has been studied using soil burial method following a procedure reported in the literature.[30]

### Electrochemical studies

Electrochemical characterization of the symmetric redox supercapacitor was carried out by cyclic voltammetry (CV), electrochemical impedance spectroscopy (EIS), and galvanostatic charge-discharge studies. The bulk ionic conductivities ($\sigma$) of the gel polymer electrolyte and the supercapacitor were determined from the impedance spectra in the frequency range between 10 mHz and 1 MHz with a perturbation of 5 mV rms in the temperature range of 298–343 K. The charge-discharge behavior of the

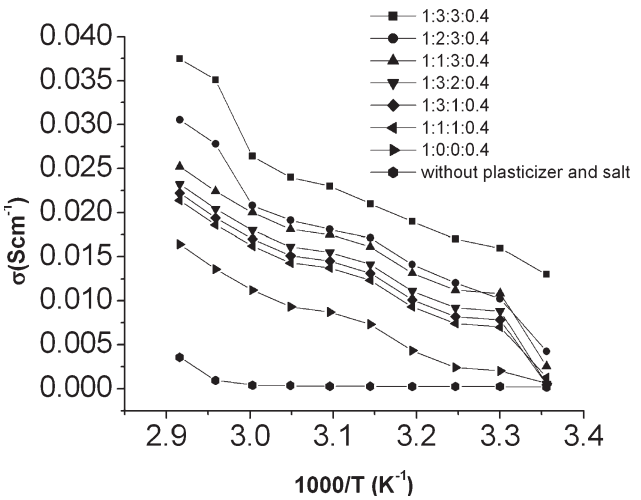


**Figure 1** Variation of conductivity of PGE films of different compositions with temperature.

fabricated super capacitor was analyzed by galvanostatic method. All the electrochemical studies were carried out using an Autolab Electrochemical System (Eco Chemie BV, The Netherlands).

### Impedance measurements

Samples were mounted on the conductivity holder with stainless steel (SS) electrodes of diameter 1 cm under spring pressure. Complex impedance data, $Z^*$ can be represented by its real, $Z_R$ and imaginary, $Z_I$ parts by the relation:

$$Z^* = Z_R + jZ_I \tag{1}$$

The relationships among complex impedance, admittance, permittivity, and electrical modulus can be found elsewhere.[31] The equations for the dielectric constant, $\varepsilon_R$, the dielectric loss, $\varepsilon_I$, the real electrical modulus, $M_R$, and the imaginary electrical modulus, $M_I$, can be shown as,

$$\varepsilon_R = \frac{Z_I}{\omega C_0 (Z_R{}^2 + Z_I{}^2)} \tag{2}$$

$$\varepsilon_I = \frac{Z_R}{\omega C_0 (Z_R{}^2 + Z_I{}^2)} \tag{3}$$

$$M_R = \frac{\varepsilon_R}{(\varepsilon_R{}^2 + \varepsilon_I{}^2)} \tag{4}$$

$$M_I = \frac{\varepsilon_I}{(\varepsilon_I{}^2 + \varepsilon_R{}^2)} \tag{5}$$

Here $C_0 = \frac{\varepsilon_0 A}{t}$ and $\varepsilon_0$ is the permittivity of the free space, $A$ is the electrolyte–electrode contact area, and $t$ is the thickness of the sample and $\omega = 2\pi f$, $f$ being the frequency in Hz.

### Electrodeposition of PPy

Py (Acros Organics) was distilled before use. SDS ($C_{12}H_{25}NaOSO_3$) was used as the surface active agent. A high-purity commercial 304 grade SS foil (thickness: 0.2 mm) was used as the substrate for PPy deposition. All solutions were prepared in double distilled water. Deposition of PPy, CV, and galvanostatic charge-discharge cycling was carried out using an AUTOLAB from Eco-Chemie. A three-electrode system was used with saturated calomel electrode as a reference electrode. A platinum foil (5 $cm^2$) was used as the counter electrode. The typical electrolyte was an aqueous solution of 0.01*M* Py and 0.1*M* SDS. PPy was electrochemically deposited onto SS electrode. Electrochemical half-cell measurements were conducted in a three-electrode cell equipped with a reference electrode (SCE), platinum foil as counter electrode, and PPy-deposited SS act as working electrode. Preliminary experiments using a polished and cleaned SS substrate indicated poor adherence of electrodeposited PPy. To improve adherence, SS sheet was subjected to sand blasting to generate noticeable rough surface and washed copiously using detergent followed by a mild etching in dilute $H_2SO_4$. A foil of 5-mm width and 4-cm length was sectioned out of a sandblasted SS sheet, 1 $cm^2$ area at one of the ends was exposed to the electrolyte, and the rest of its length was used as a tag for taking electrical contacts. The SS substrate was again washed thoroughly, rinsed with acetone, and dried in vacuum at ambient temperature for about 30 min and weighed before electrodeposition of PPy. After the deposition, the electrode was separated from the cell, rinsed with double distilled water, dried at 50°C, and weighed. The surface morphology of the PPy electrodes was determined using a scanning electron microscope (SEM).

### Fabrication of symmetrical (p/p) super capacitor cell

The capacitor cells were constructed with a $LiClO_4$ salt containing chitosan PGE sandwiched between two symmetrical PPy-deposited electrodes. Electrochemical characterization of the PPy-deposited electrode was carried out by CV, EIS, and galvanostatic charge-discharge studies.

## RESULTS AND DISCUSSION

### Ionic conductivity studies

The bulk ionic conductivities ($\sigma$) of the solid polymer electrolytes have been determined from the complex impedance spectra using the equation, $\sigma = \frac{L}{RA}$, where $L$, $R$, and $A$ are the thickness, bulk resistance, and area of the solid polymer electrolyte,

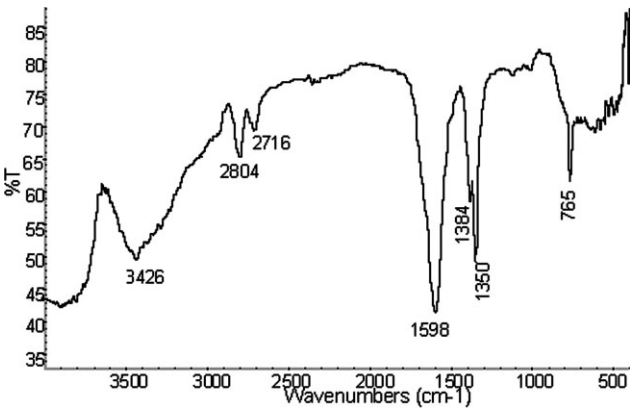


**Figure 2** FTIR spectrum of neat chitosan.

respectively. The bulk resistance was calculated from the high frequency intercept on the real impedance axis of the Nyquist plot.[32] The temperature dependence of conductivity for the chitosan PGE has been shown in Figure 1. The plot shows that as temperature increases, the conductivity increases. This is due to the increased mobility of the ions at higher temperatures. As there is no sudden change in the value of conductivity with temperature, it may be inferred that these complexes do not undergo any phase transitions within the temperature range investigated. Activation energy, $E_A$, was calculated from the slope of the log σ versus $10^3/T$ graph. This is based on the Arrhenius rule, $\sigma = \sigma_0 \exp(-E_A/kT)$, where $\sigma_0$ is the pre-exponential factor, $E_A$ is activation energy, $k$ is Boltzmann constant, and $T$ is absolute temperature. The calculated activation energy was found to be 0.9 eV. Further, it is also expected that lithium salt can have specific interactions such as hydrogen bonding with chitosan. To confirm the presence of hydrogen bonding in the PGE, FTIR spectra of neat chitosan and lithium salt-doped plasticized chitosan films have been measured at room temperature. Although the changes in energies, bond lengths, and electron densities with the formation of hydrogen bonds are actually quite small and about two to three orders of magnitude smaller than typical chemical changes, FTIR spectroscopy is very sensitive to the formation of hydrogen bond.[33] If the groups involved in the hydrogen bond formation in a given system are carbonyl and hydroxyl moieties, then the vibration frequencies of both the groups are expected to show a red shift because of hydrogen bond formation compared with the noninteracting group frequencies. The IR spectra of neat chitosan and that with plasticizer and lithium salt have been shown in Figures 2 and 3. The absorption band at 3426 $cm^{-1}$ is attributed to the OH stretching frequency of chitosan. This band has been red shifted to 3408 $cm^{-1}$ in chitosan with lithium salt. This may be due to the hydrogen bonding interaction between perchlorate ions of the salt and OH groups of chitosan. Such behaviors have also been reported in the literature.[30,34]

### Soil burial degradation study

Chitosan is a well-known biodegradable material. Lithium perchlorate being an ionic compound is also expected to degrade easily in the environment. Hence, the PGE based on chitosan–lithium salt is also expected to undergo biodegradation. However, to experimentally confirm this proposition, a short-term study for a period of 30 days has been conducted on the soil degradation behavior of the PGE. Although long-term studies are more useful in characterizing the soil degradation of matrices (e.g., for an year or 2), the short-term study does give an insight into the biodegradation behavior and can be used for a rapid evaluation of biodegradability of polymeric materials.[35] In this study, the PGE films showed a weight loss of about 60% (Fig. 4) in 30 days. This result confirms the proposition and indicates that the PGEs are excellent biodegradable materials. The PGE exposed to soil might have initially undergone biodegradation, where microorganisms consume the natural cellulose component. Consequently, the oxygen can attack the newly generated surface with the formation of peroxides, hydroperoxides, oxides, etc., which promote the scission of polymeric chains into small fragments more susceptible to the attack of microorganisms.[35–37] Soil bacteria and fungi might be responsible for the degradation.[37]

### Dielectric studies

The conductivity behavior of the PGEs can be understood from the dielectric studies.[38] The dielectric constant is a measure of stored charge. The variation of dielectric constant and dielectric loss as a function of temperature for samples with and without

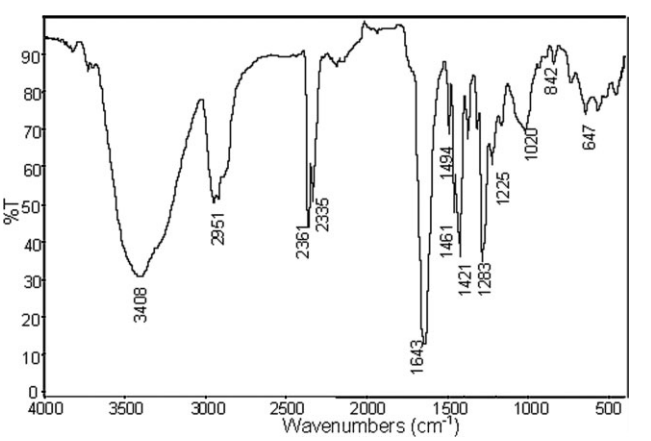


**Figure 3** FTIR spectrum of lithium salt-doped plasticized chitosan.

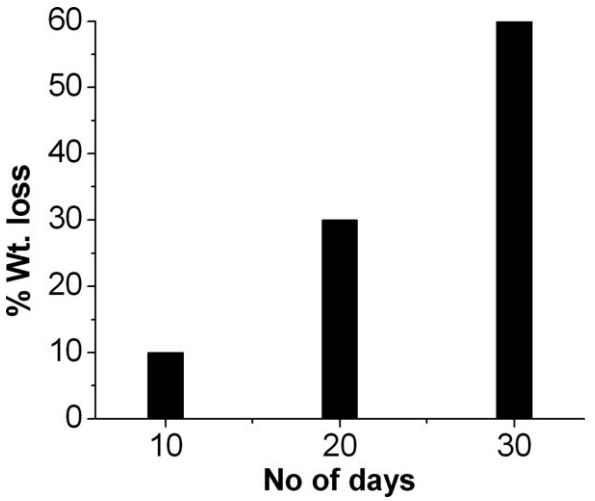


**Figure 4** Soil burial degradation of PGE.

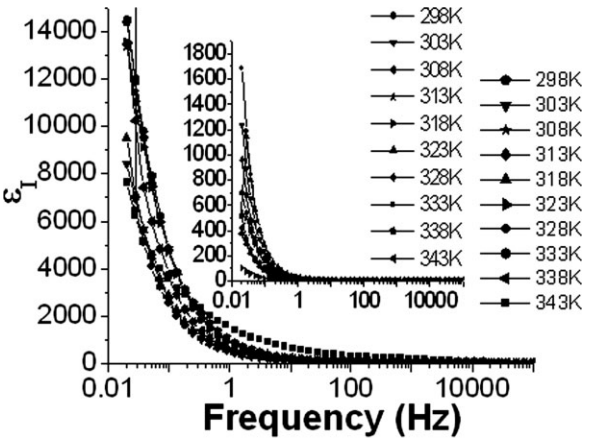


**Figure 6** Plots of dielectric loss versus frequency at different temperatures (inset: without plasticizer).

plasticizer is shown in Figures 5 and 6, respectively. There are no appreciable relaxation peaks observed in the frequency range used in the study. Both dielectric constant and dielectric loss increase sharply at low frequencies, indicating that electrode polarization and space charge effects have occurred confirming non-Debye dependence.[39,40] On the other hand, at high frequencies, periodic reversal of the electric field occurs so fast that there is no excess ion diffusion in the direction of the field. Polarization due to charge accumulation decreases, leading to the observed decrease in dielectric constant and dielectric loss.[38–41] The dielectric constant and dielectric loss increase at higher temperatures because of the higher charge carrier density. As temperature increases the degree of salt dissociation and redissociation of ion aggregates increases, resulting in an increase in the number of free ions or charge carrier density. The dielectric constant, $\varepsilon_R$, versus frequency plots for the PGE film are shown in Figure 5. The inset shows $\varepsilon_R$ values for the film without plasticizer. $\varepsilon_R$ has high values at low frequencies. This implies that the mobile ions tend to get accumulated at low frequencies. The value of $\varepsilon_R$ for the PGE film is much (up to 20 times) higher than that without plasticizer. The dielectric constant plays a fundamental role in the ability of a polymer to dissolve salts. With increasing plasticizer content and for a fixed frequency, the value of $\varepsilon_R$ for the film increases. This shows that the plasticizer has increased the dielectric constant of the biopolymer and increased its ability to dissolve the salt. Therefore, the number of mobile ions in the sample increases and because the conductivity is proportional to the number of mobile ions, the conductivity is therefore increased. It is quite obvious that salt is the agent responsible for conductivity of the PGE film as other components of the film do not have such species. The role of the plasticizer here is to help the salt to dissociate into mobile ions or to increase the mobility of the ions so that the conductivity of film increases. The effect of the plasticizer in increasing the ability of a polymer to dissociate the salt has also been observed by other workers. Alternatively, plasticization can also increase ionic mobility by reducing the potential barrier to ionic motion as a result of the decreasing cation–anion coordination of the salt.[42,43] Because no significant relaxation peaks have been observed in the dielectric loss-frequency spectrum in Figure 5, it is inferred that residual water does not contribute toward conductivity enhancement. The variations of real ($M_R$) and imaginary ($M_I$) parts of electrical modulus for PGE film and that without plasticizer are depicted in Figures 7 and 8, respectively. Both $M_R$ and $M_I$ show an increase at the higher frequency end and exhibits a long tail feature at low frequency end. This indicates that the material is very capacitive in nature.[44]

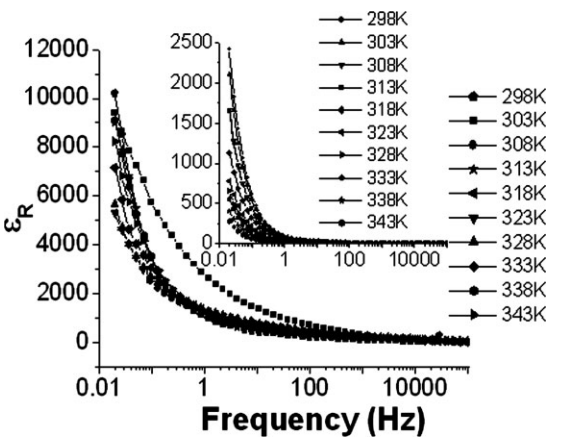


**Figure 5** Plots of dielectric constant versus frequency at different temperatures (inset: without plasticizer).

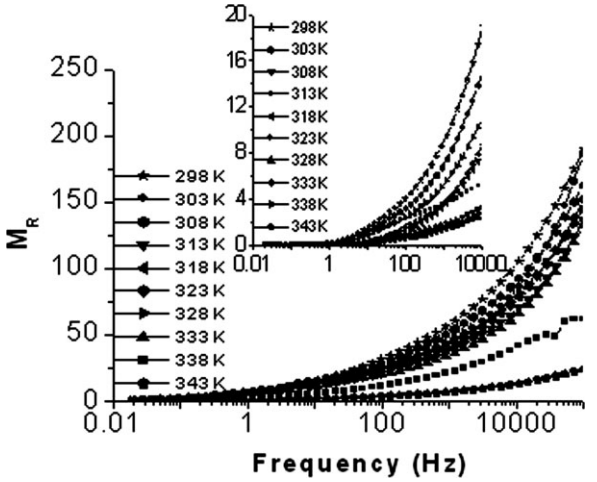


**Figure 7** Plots of real part of electric modulus versus frequency at different temperatures (inset: without plasticizer).

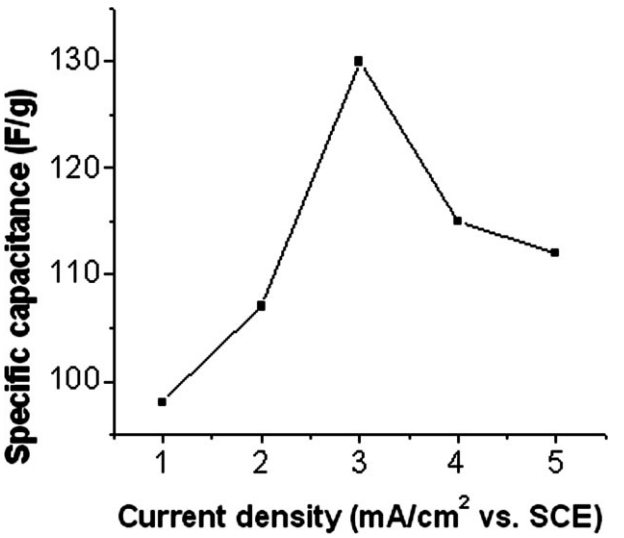


**Figure 9** Variation of specific capacitance of PPy/SS electrode with current density.

### Electrode studies

Electrochemical oxidation of the monomer could be accomplished by galvanostatic method. Preliminary experiments were carried out by depositing PPy galvanostatically on SS substrates. Figure 9 shows the variation of specific capacitance (SC) of the formed electrode at different current densities. SC decreased from 130 F $g^{-1}$ at 3 mA $cm^{-2}$ to 90 F $g^{-1}$ at 11 mA $cm^{-2}$. This may be due to the formation of bulk deposits with lesser surface area at higher current densities. This in turn can lead to lower SC. Hence, further electrochemical experiments were done at a fixed current density of 3 mA $cm^{-2}$.

The influence of SDS concentration on the electrode properties has been studied. PPy/SS electrodes have been prepared in 0.01*M* pyrrole and 0.1*M* $H_2SO_4$ medium with varying concentration of SDS in the range of 0.001–0.3*M* at a current density of 3 mA $cm^{-2}$ for 500 s. The Nyquist plots for the deposition process have been shown in Figure 10. It is evident from the plot that the resistance of PPy electrode is minimum when SDS concentration is 0.01*M*. The charges involved in the doping–undoping processes within the conducting polymers strongly depend on the nature of the electrolyte, and hence, SC values also differ from electrolyte to electrolyte. Capacitance behavior of PPy/SS electrodes here has been studied by subjecting them to CV and galvanostatic charge-discharge cycling. The variation of SC with $H_2SO_4$ concentrations is shown in Figure 11. As can be seen from the plot, there is a steady decrease in SC from 130 F $g^{-1}$ for the PPy/SS electrodes prepared in 0.1*M* $H_2SO_4$ to about 80 F $g^{-1}$ for the

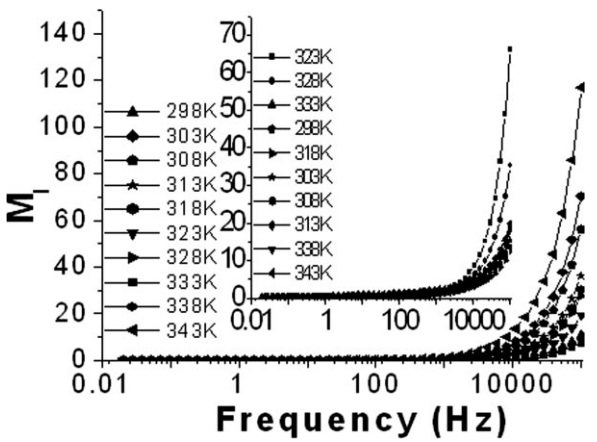


**Figure 8** Plots of imaginary part of electric modulus versus frequency at different temperatures (inset: without plasticizer).

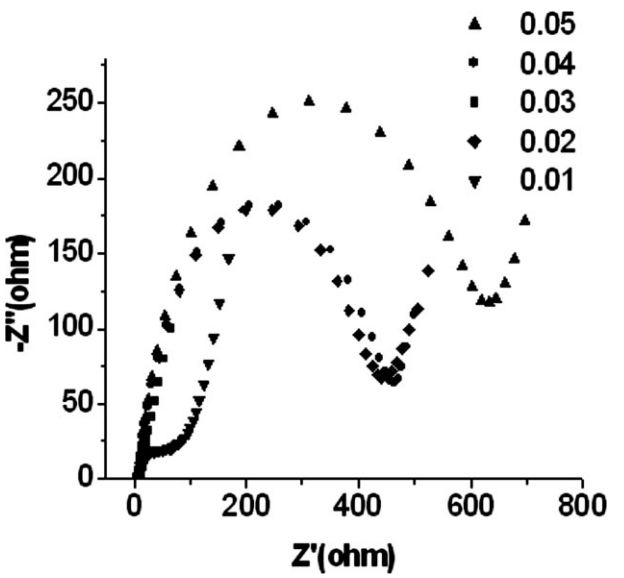


**Figure 10** Nyquist plots for PPy depositon.

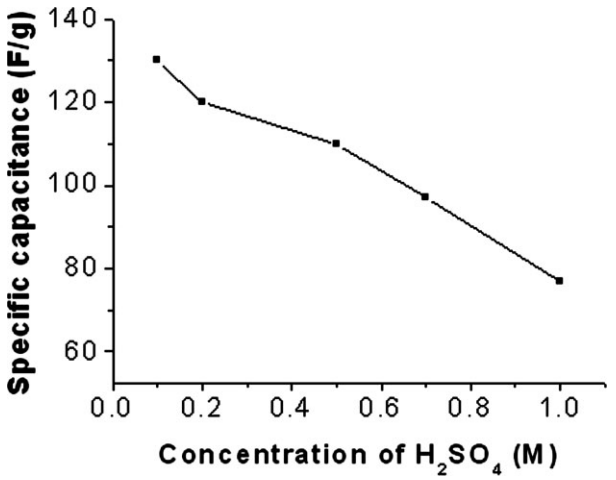


**Figure 11** Variation of specific capacitance with $H_2SO_4$ concentration.

electrode prepared in 1*M* $H_2SO_4$. Thus, 0.1*M* $H_2SO_4$ was used for preparing PPy/SS electrodes for rest of the studies. In a similar way, PPy/SS electrodes have been prepared in 0.1*M* $H_2SO_4$ by varying the concentration of SDS from 0.001 to 0.3*M*, and SC values have been measured. The variation of SC with concentration of SDS is shown in Figure 12. A maximum SC of 130 F $g^{-1}$ has been obtained when SDS concentration was 0.01*M*. There was a decrease in SC either by decreasing or increasing the concentration of SDS from 0.01*M*. The increase in SC up to 0.01*M* is due to increased rate of formation of PPy facilitated by SDS micelle-pyrrole cation-free radicals. When the SDS concentration exceeds 0.01*M*, which is also the monomer concentration in the system, the surface concentration of uncomplexed micells increases. This results in the decrease in the rate of formation of PPy and hence also the SC of

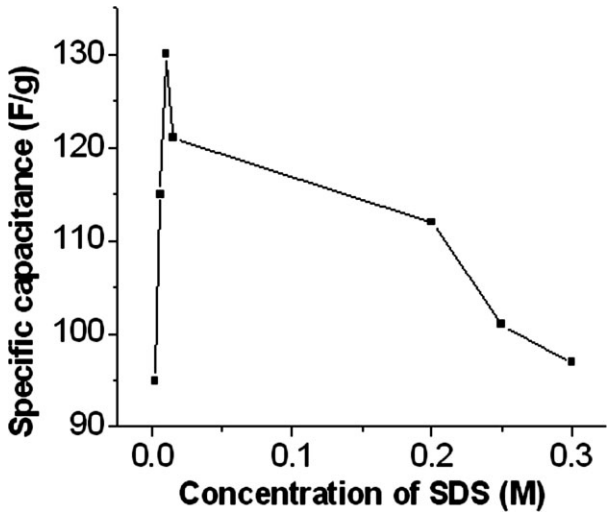


**Figure 12** Dependence of specific capacitance on SDS concentration.

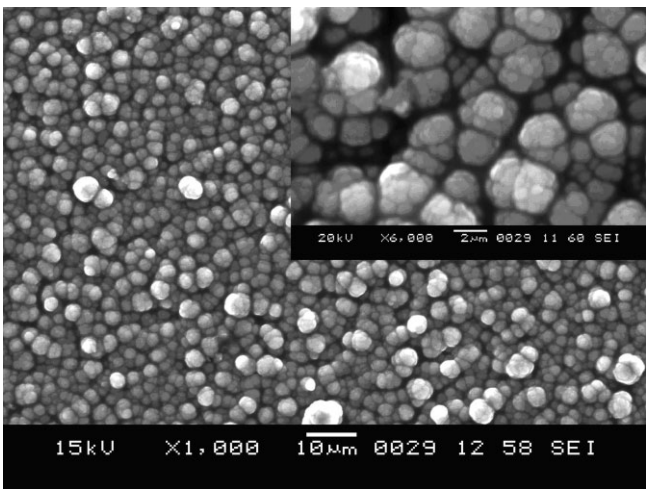


**Figure 13** SEM image of PPy/SS electrode surface prepared at 0.01*M* SDS concentration (inset: magnified view of the surface).

the electrode. The higher concentration of SDS can also lead to the formation of unfavorable morphological structures with less surface area. Figure 13 shows SEM micrograph of the electrode surface prepared at 0.01*M* SDS concentration. The image reveals globulous surface morphology with higher surface area. Figure 14 shows SEM image of the electrode prepared in 1*M* SDS. As can be seen from the image, the surface is quite irregular compared with the former. The deposit is of less surface area and less adherent to the electrode surface. Thus, a decrease in porosity and surface area resulted by the increase in SDS concentration accounts for a decrease in SC of PPy/SS electrodes. Similar observations have also been reported by Patra and Munichandraiah.[45] Hence, SDS concentration has been fixed at 0.01*M* for all other experimental runs.

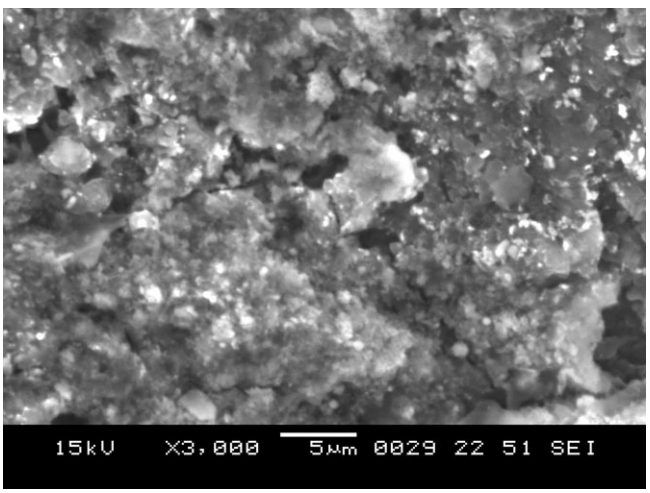


**Figure 14** SEM image of PPy/SS electrode surface prepared at 0.01*M* SDS concentration.

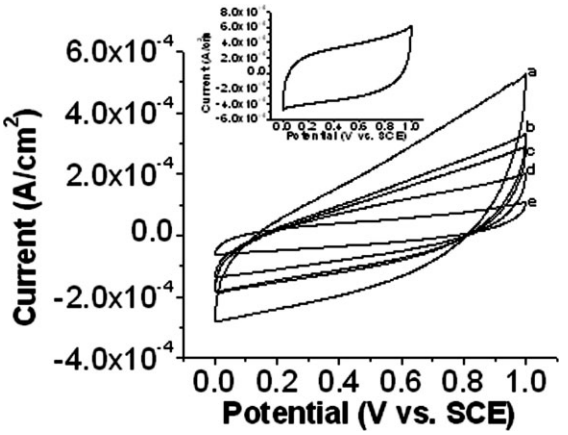


**Figure 15** CVs of polypyrrole deposited on SS electrodes at scan rates. (a) 50 mV $s^{-1}$, (b) 25 mV $s^{-1}$, (c) 20 mV $s^{-1}$, (d) 10 mV $s^{-1}$, and (e) 5 mV $s^{-1}$(inset: CV of the electrode at 25 mV $s^{-1}$).

### Supercapacitor studies

CVs for PPy deposited on SS electrode at various sweep rates are shown in Figure 15. The single-electrode responses clearly show the capacitive characteristics as well as the corresponding redox features of PPy under doping and dedoping. The CV for the supercapacitor cell fabricated using the biodegradable electrolyte is shown in Figure 16. The CV exhibits the typical capacitive features and the observed patterns are in conformity with that reported.[46–49]

The capacitance values for the symmetric capacitor (Table I) have been calculated[46] from the CVs using the equation: $C = i/s$, where $s$ is the potential sweep rate and $i$ is the average current. SC of 130 F $g^{-1}$ was obtained for the single electrode at the sweep rate of 10 mV $s^{-1}$, and the same for the fabricated biodegradable gel polymer electrolyte-based supercapacitor was 80 F $g^{-1}$. This value is also comparable to that reported.[47–49] The reduction in the capacitance in the case of supercapacitor is quite normal, because in the supercapacitor fabrication the two PPy electrodes constitute the electrochemical configuration of a parallel plate condenser connected in series. The equivalent circuit for the fabricated supercapacitor is similar to the one with a DLC and a redox capacitor in parallel combination.[50] Hence, the resistance and capacitance values have also been calculated from this equivalent circuit and from AC impedance spectroscopy. The values from both the methods are found to be comparable. The specific energy (SE, Wh $g^{-1}$), specific power (SP, W $g^{-1}$), coulombic efficiency ($N$%), and IR drop of the supercapacitor during cyclings have also been estimated using galvanostatic method. The values are also comparable to that of reported supercapacitors.[51] The values are shown in Table II.

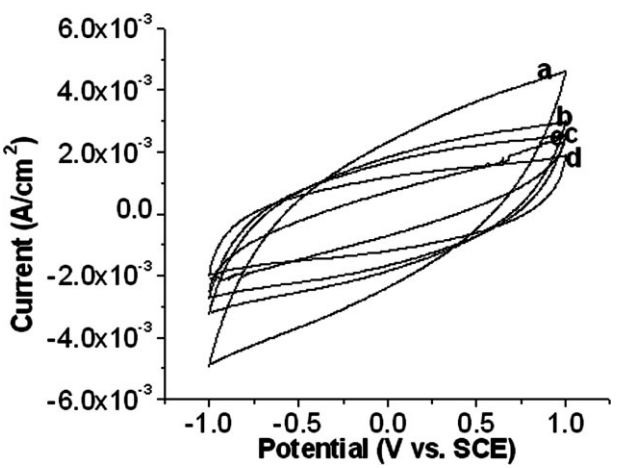


**Figure 16** CVs of the fabricated p/p polypyrrole symmetric supercapacitor using PGE at scan rates. (a) 50 mV $s^{-1}$, (b) 25 mV $s^{-1}$, (c) 20 mV $s^{-1}$, (d) 10 mV $s^{-1}$, and (e) 5 mV $s^{-1}$.

**TABLE I**
**Specific Capacitance Values of the PPy/SS Single Electrode and the Supercapacitor Based on the Gel Polymer Electrolyte**

| Serial no. | Materials | Scan rate (mV $s^{-1}$) | Specific capacitance (F $g^{-1}$) |
|---|---|---|---|
| 1 | Polypyrrole | 10 | 120 |
| | | 20 | 90 |
| | | 25 | 80 |
| | | 50 | 70 |
| 2 | Symmetrical supercapacitor | 10 | 80 |
| | | 20 | 57 |
| | | 25 | 35 |
| | | 50 | 27 |

The AC impedance response of capacitor is shown in Figure 17. A semicircle is obtained at high frequency range and almost a straight line in the low frequency region. The capacitance values increase at low frequencies because of a larger number of ions moving which cause a decrease in the bulk resistance of the capacitor. The semicircle results from the parallel combination of resistance and capacitance and the linear region is due to Warburg impedance. In the low frequency region, the linear region leans more toward imaginary axis and this indicated good capacitive behavior.[50] These electrochemical impedance data have been analyzed by plotting the normalized imaginary part /Q///S/ and real part /P///S/ of the complex power ($S$) versus frequency

**TABLE II**
**Supercapacitor Parameters**

| Cycle no. | SP (W $g^{-1}$) | SE (Wh $g^{-1}$) | $N$% | ESR (Ω) | IR drop (V) |
|---|---|---|---|---|---|
| 1 | 0.22 | 35 | 98 | 10 | 0.02 |
| 1000 | 0.22 | 35 | 95 | 12 | 0.03 |

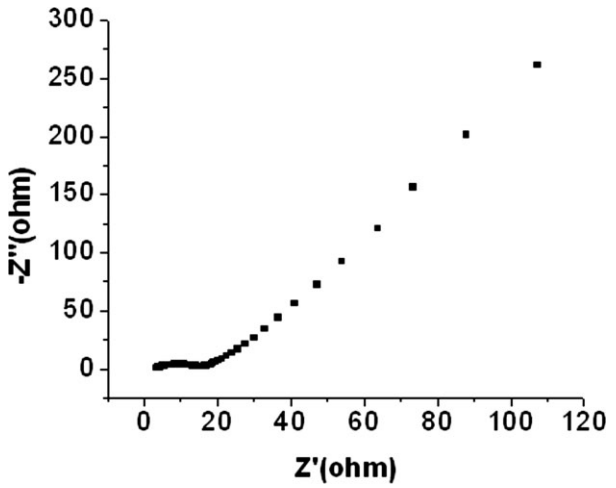


**Figure 17** AC impedance spectra of the supercapacitor.

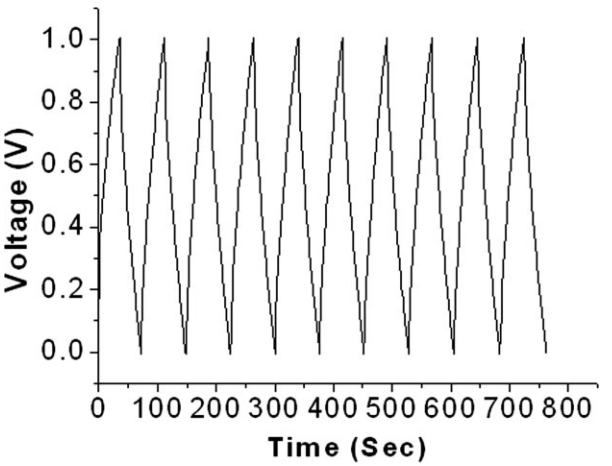


**Figure 19** Galvanostatic charge–discharge plots for the supercapactior for the first 10 cycles.

and are shown in Figure 18. The relaxation time constant of the supercapacitor determined from these data was found to be 2 s. The time constant, $\tau_0$, represents a transition for the supercapacitor between a resistive behavior for frequency higher than $1/\tau_0$ and a capacitive behavior for frequency lower than $1/\tau_0$.

Figure 19 shows the charge-discharge profile of the supercapacitor as measured by galvanostatic method at a constant current density of 2 mA $cm^{-2}$ between 0 and 1.0 V, for the first 10 cycles. From the figure, it can be seen that the voltage of the capacitor varies almost linearly with time during both charging and discharging processes for various cycles. It is evident from the figure that the charging time and also discharging time remained constant with increasing number of cycles. However, there may be a slightly higher voltage drop and decrease in the charging and discharging time with cyclings as well as with current density beyond 1000 cycles or so because of the degradation possibility of the cell redox activity.[50,51] The coulombic efficiency of the supercapacitor calculated from charge–discharge cyclings is also high in the range of 98–99%. In the absence of the lithium salt, the fabricated supercapacitor showed a coulombic efficiency of around 85–86%, indicating the influence of lithium salt in supercapacitor performances.

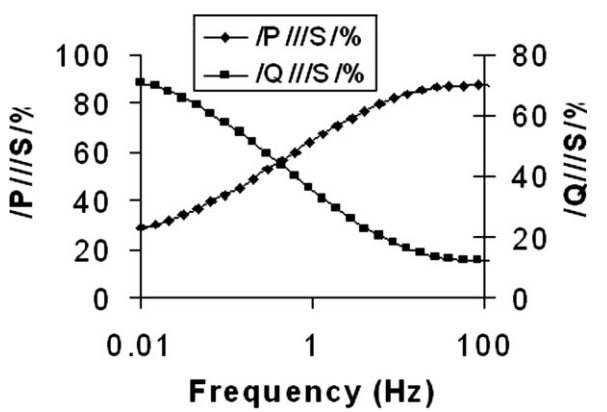


**Figure 18** Plots of normalized reactive power /Q///S/% and active power /P///S/% versus frequency (Hz) supercapacitor.

## CONCLUSIONS

In this study, possibility of producing a biodegradable PGE based on chitosan–lithium perchlorate complex has been investigated. The conductivity of the plasticized chitosan-salt complexes is due to the salt and can be enhanced by plasticization. Highest conductivity obtained for the PGE film is found to be $5.5 \times 10^{-3}$ S $cm^{-1}$. Soil burial degradation analysis of the PGE suggested that the material has excellent biodegradation characteristics. The electrochemical impedance studies reveal that the concentration of surfactant and supporting electrolyte as well as the current density influence the SC of the formed electrodes. The p/p PPy symmetric supercapacitor fabricated using this biodegradable material showed a capacitance of 80 F $g^{-1}$ and was stable during cyclings with a coulombic efficiency of about 99%. Hence, the study demonstrates the successful preparation of a biodegradable gel polyelectrolyte for use in supercapacitors.

MSK is grateful to NITK Surathkal for the award of a Research Fellowship.

## References

1. Wan, Y.; Creber, K. A. M.; Peppley, B.; Mui, V. T. Polymer 2003, 44, 1057.
2. Muzzarelli, R. A. A. Natural Chelating Polymers: Alginic Acid, Chitin and Chitosan; Pergamon Press: Oxford, 1973.
3. Mohamed, N. S.; Subban, R. H. Y.; Arof, A. K. J Power Sources 1995, 56, 153.

4. Yahya, M. Z. A.; Arof, A. K. Eur Polym J 2003, 39, 897.
5. Yahya, M. Z. A.; Arof, A. K. Carbohydr Polym 2004, 55, 95.
6. Maccallum, J. R.; Vincent, C. A., Eds. Polymer Electrolyte Review; Elsevier: London, 1987–89; Vol. 1/2.
7. Dias, F. B.; Plomp, L.; Velduis, J. B. J. J Power Sources 2000, 88, 169.
8. Matsuda, Y.; Inoue, K.; Takeuchi, H.; Okuhama, Y. Solid State Ionics 1998, 113, 103.
9. Ishikawa, M.; Ihara, M.; Morita, M.; Matsuda, Y. Electrochim Acta 1995, 40, 2217.
10. Conway, B. E. Electrochemical Supercapacitors, Scientific Fundamentals and Technological Applications; Kluwer Academic Publishers: New York, 1999.
11. Frackowiak, E.; Bequin, F. Carbon 2001, 39, 937.
12. Gamby, J.; Taberna, P. L.; Simon, P.; Fauvarque, J. F.; Chesneau, M. J Power Sources 2001, 101, 109.
13. Mayer, S. T.; Pekala, R. W.; Kaschmitler, J. L. J Electrochem Soc 1993, 140, 446.
14. Wang, T.; Zhang, S. Q.; Guo, Y. Z.; Shen, J.; Attia, S. M.; Zhou, B.; Zeng, G. Z.; Gui, Y. S. J Electrochem Soc 2001, 148, D75.
15. Frackowiak, E.; Meternier, K.; Bertagna, V.; Bequin, F. Appl Phys Lett 2000, 77, 2421.
16. Frackowiak, E.; Jurewicz, K.; Delpeux, S.; Bequin, F. J Power Sources 2001, 97, 822.
17. Gupta, P. N.; Singh, K. P. Solid State Ionics 1996, 86, 319.
18. Yong-Gang, W.; Xiao-Gang, Z. Electrochim Acta 2004, 49, 1957.
19. Guinot, S.; Salmon, E.; Renneau, J. F.; Fauvarque, J. F. Electrochim Acta 1998, 43, 1163.
20. Yang, C. C. J Power Sources 2002, 109, 22.
21. Iwakura, C.; Nohara, S.; Furukawa, N.; Inoue, H. Solid State Ionics 2002, 148, 487.
22. Iwakura, C.; Wada, H.; Nohara, S.; Furukawa, N.; Inoue, H.; Morita, M. Electrochem Solid-State Lett 2003, 6, A37.
23. Feuillade, G.; Perche, P. J Appl Electrochem 1975, 5, 63.
24. Bohnke, O.; Frand, G.; Rezrazi, M.; Rousselot, C.; Truche, C. Solid State Ionics 1993, 66, 97.
25. Appetecchi, G. B.; Croce, F.; Scrosat, B. Electrochim Acta 1995, 40, 991.
26. Gospondinova, N.; Fereleme-Zyan, L. Prog Polym Sci 1998, 23, 1443.
27. Skothemin, T.; Elsenbaumer, R. Hand Book of Conductive Polymers; Marcel Dekker: New York, 1998.
28. Shimdzu, T.; Ohtani, A.; Honda, K. J Chem Soc Jpn 1988, 61, 2885.
29. Zhong, C.; Doblhofer, K. Electrochim Acta 1990, 35, 1971.
30. Selva Kumar, M.; Krishna Bhat, D. J Appl Polym Sci 2008, 110, 594.
31. Macdonald, J. R., Ed. Impedance Spectroscopy; Wiley: New York, 1987.
32. Choudhury, N. A.; Shukla, A. K.; Sampath, S.; Pitchumani, S. J Electrochem Soc 2006, 153, A614.
33. He, Y.; Zhu, B.; Inoue, Y. Prog Polym Sci 2004, 29, 1021.
34. Coleman, M. M.; Painter, P. C. Prog Polym Sci 1995, 20, 1.
35. Krishna Bhat, D.; Selvakumar, M. J Polym Environ 2006, 14, 385.
36. Chandra, R.; Rustgi, R. Prog Polym Sci 1998, 23, 1273.
37. Okada, M.; Yamada, M.; Yokoe, M.; Aoi, K. J Appl Polym Sci 2001, 81, 2721.
38. Ramesh, S.; Yahya, A. K.; Arof, A. K. Solid State Ionics 2002, 152, 291.
39. Qian, X.; Gu, N.; Cheng, Z.; Yang, X.; Wang, E.; Dong, S. Electrochim Acta 2001, 46, 1829.
40. Govindaraj, G.; Bhaskaran, N.; Shahi, K.; Monoravi, P. Solid State Ionics 1995, 76, 47.
41. Ramesh, S.; Arof, A. K. J Power Sources 2001, 99, 41.
42. Forsyth, M.; Meakin, P. M.; Macfarlane, D. R. Electrochim Acta 1995, 40, 2339.
43. Forsyth, M.; Macfarlane, D. R.; Meakin, P.; Smith, M. E.; Bastow, T. J. Electrochim Acta 1995, 40, 2343.
44. Osman, Z.; Ibrahim, Z. A.; Arof, A. K. Carbohydr Polym 2001, 4, 167.
45. Patra, S.; Munichandraiah, N. J Appl Polym Sci 2007, 106, 1170.
46. Muthulakshmi, B.; Kalpana, D.; Pitchumani, S.; Renganthan, N. G. J Power Sources 2005, 158, 1533.
47. Mastragostino, M.; Arbizzani, C.; Soavi, F. Solid State Ionics 2002, 148, 493.
48. Krishna Bhat, D.; Selva Kumar, M. J Mater Sci 2007, 42, 8158.
49. Selva Kumar, M.; Krishna Bhat, D. J Appl Polym Sci 2008, 107, 2165.
50. Taberna, P. L.; Simon, P.; Fauvarque, J. F. J Electrochem Soc 2003, 150, A292.
51. Conway, B. E. Electrochemical Supercapacitors: Scientific Fundamentals and Technological Applications; Kluwer Academic Publishing: New York, 1999.